Nanoscale

Cite this: *Nanoscale*, 2011, **3**, 4515

www.rsc.org/nanoscale

FEATURE ARTICLE

Carbon-based layer-by-layer nanostructures: from films to hollow capsules

Jinkee Hong,†[a] Jung Yeon Han,[a] Hyunsik Yoon,[a] Piljae Joo,[b] Taemin Lee,[b] Eunyong Seo,[b] Kookheon Char*[a] and Byeong-Su Kim*[b]

Received 4th June 2011, Accepted 11th July 2011
DOI: 10.1039/c1nr10575b

Over the past years, the layer-by-layer (LbL) assembly has been widely developed as one of the most powerful techniques to prepare multifunctional films with desired functions, structures and morphologies because of its versatility in the process steps in both material and substrate choices. Among various functional nanoscale objects, carbon-based nanomaterials, such as carbon nanotubes and graphene sheets, are promising candidates for emerging science and technology with their unique physical, chemical, and mechanical properties. In particular, carbon-based functional multilayer coatings based on the LbL assembly are currently being actively pursued as conducting electrodes, batteries, solar cells, supercapacitors, fuel cells and sensor applications. In this article, we give an overview on the use of carbon materials in nanostructured films and capsules prepared by the LbL assembly with the aim of unraveling the unique features and their applications of carbon multilayers prepared by the LbL assembly.

[a]*The National Creative Research Initiative Center for Intelligent Hybrids, The WCU Program of Chemical Convergence for Energy & Environment, School of Chemical and Biological Engineering, Seoul National University, Seoul, 151-744, Korea. E-mail: khchar@plaza.snu.ac.kr*
[b]*Interdisciplinary School of Green Energy, KIER-UNIST Advanced Center for Energy and School of NanoBioscience and Chemical Engineering, Ulsan National Institute of Science and Technology (UNIST), Ulsan, 689-798, Korea. E-mail: bskim19@unist.ac.kr*
† Current address: Department of Chemical Engineering, Massachusetts Institute of Technology, 77 Massachusetts Avenue, Cambridge, MA 02139 USA.

Jinkee Hong

Dr Jinkee Hong received his PhD in Chemical and Biological Engineering under the direction of Prof. Kookheon Char at Seoul National University. His PhD research has focused on the self-assembly of nano-objects with polymeric materials for multifunctional thin films. Currently, he is a postdoctoral researcher at the Massachusetts Institute of Technology (MIT) under the supervision of Prof. Paula T. Hammond working in the area of building platforms for both biomedical and energy applications.

Kookheon Char

Dr Kookheon Char is a professor of Chemical and Biological Engineering at Seoul National University. He studied chemical engineering at Seoul National University and KAIST. After his PhD study at Stanford University in 1989, he worked for IBM for his postdoctoral research. Since 1991, he worked at Seoul National University as a professor. He is now serving as the director of the National Creative Research Initiative Center for Intelligent Hybrids, funded by the National Research Foundation of Korea. He was awarded the Gutenberg Research Award from Johannes Gutenberg University and the 12th National Academy of Engineering of Korea Young Engineer Award. His research and educational program emphasizes the use of macromolecular aspects in the study and development of novel materials and strategies, including the molecular design and synthesis of self-assembling polymeric materials and nanoscale objects and building smart film systems for energy and medicine applications.

1. Introduction

The creation of nanoscale materials with various compositions, structures, and dimensions is of tremendous interest due to their unique potential in many fields of science and technology.[1,2] Various types of nanosized materials including inorganic, organic, polymeric, and biological materials can be synthesized or prepared with precise control over their nanoscopic features such as size, shape, and composition, which will eventually lead to the fine tuning of their corresponding optical, electrical, mechanical, and biological properties.[3] Although great achievements have thus far been made in the synthesis and characterization of individual nanoscale materials, it is still challenging to design and control their assembly at various length scales to transfer from nanoscale properties to macroscale structures. Because their collective properties in macroscopically assembled structures are significant both for fundamental understanding and practical applications, it is essential to develop a method of the assembly of nanoscale objects in a controlled and predictable manner.[4,5]

The layer-by-layer (LbL) assembly, first introduced by Iler[6] and later by Decher,[7] is by far one of the most versatile methods to assemble multifunctional nanoscale materials with nanometre-scale control over composition and structure.[8] Beyond the traditional use of polymers in the LbL assembly, it now accommodates diverse nanostructures, including nanoparticles,[9] carbon nanotubes,[10] and biomolecules,[11] each with distinct structure, composition and function depending on the choice of materials and controlling the sequence of layering. Due to its simplicity and versatility, the LbL assembly has rapidly emerged as a platform technique for the assembly of hybrid nanomaterials as 2-dimensional thin film coatings with desired architectures of functional hybrid materials. It can even be extended to the coating of 3-dimensional objects for functional capsules loaded with active molecules of interest.[12–15]

Owing to their unique physical, chemical, and mechanical properties, carbon nanomaterials such as fullerenes (0D),[16] carbon nanotubes (1D),[17,18] and graphenes (2D)[19–21] are offering promising opportunities in the design of functional thin films including catalytic membranes, biosensors, energy and electronic devices, and mechanical thin film applications (Fig. 1).

As the applications of carbon nanomaterial-based functional structures become more diverse and sophisticated, it is critical to develop efficient strategies for controlling the architecture, geometry, and thickness of the films to tailor the properties and functions. Although there are other ways of creating thin films of carbon nanomaterials such as simple filtration or chemical vapor deposition, recent progress made with integrating carbon nanomaterials into the LbL assembly is gathering new perspectives in a variety of research areas.

Because of the simplicity and robustness of the LbL assembly, there already exist a series of excellent reviews on the LbL as well as their diverse applications.[23–27] To our knowledge, however, there are few reviews based on the carbon nanomaterial-based LbL assembly.[28] In this feature article, therefore, we provide a short overview of general aspects of the LbL assembly with particular emphasis on the recent advancements in the synthesis and LbL applications of carbon-based nanomaterials. We discuss the carbon-based LbL assembly based on dimensions, such as 2-dimensional thin films and 3-dimensional substrate-free capsules. Accordingly, this article is divided into two sections with subsections covering different applications. Finally, we will highlight the perspectives of the emerging field of the carbon-based LbL assembly for future applications.

2. Basics of LbL assembly

2.1. A brief overview of basic principles in LbL assembly

The basic idea of repetitive adsorption of oppositely charged species dates back to the seminal experiment of Iler in 1964, which demonstrated the deposition of oppositely charged silica and alumina particles on a substrate.[29] With the revolutionary development of characterization tools for nanoscale objects since then, the concept of repetitive adsorption was revived in the early 20th century by Decher who demonstrated the possibility of making thin films from the alternate adsorption of oppositely charged polyelectrolytes (Fig. 2).[7] The LbL assembly has rapidly drawn a great deal of attention in many fields of science and technology with a growing community over the disciplines, and the year 2011 will mark the 20th anniversary of the LbL assembly after its official debut in 1991. With its versatility and simplicity, the LbL approach has now been commercialized in microelectronics and the metal-coating industry.

The simplest analogy of the LbL assembly on a substrate is the formation of solution complexes, which are often insoluble in solution, between two oppositely charged polyelectrolytes. Similarly, the LbL deposition is based on the self-diffusion process in which charged materials are adsorbed onto the substrate based on complementary attractions. While polymer chains self-diffuse into the LbL assembly film, the assembled thin films lead to the formation of additional complexes in the thin films, hence contributing to the overall entropic gain of polymeric structures.[30] Another important feature of the LbL assembly, which is often

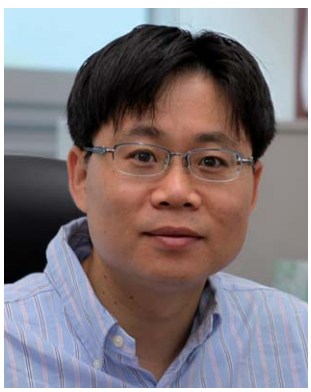

Byeong-Su Kim

Dr Byeong-Su Kim is an assistant professor of Interdisciplinary School of Green Energy at Ulsan National Institute of Science and Technology (UNIST) since 2009. He received his BS and MS degrees in chemistry from Seoul National University. In 2007, he received his PhD in polymer and nanomaterial chemistry from University of Minnesota. From 2007 to 2009, he worked as a postdoctoral research associate at the Massachusetts Institute of Technology (MIT) under the supervision of Prof. Paula T. Hammond. His current research interests include the chemistry of nanomaterials and the development of soft and hybrid nanomaterial for energy and biomedical applications.

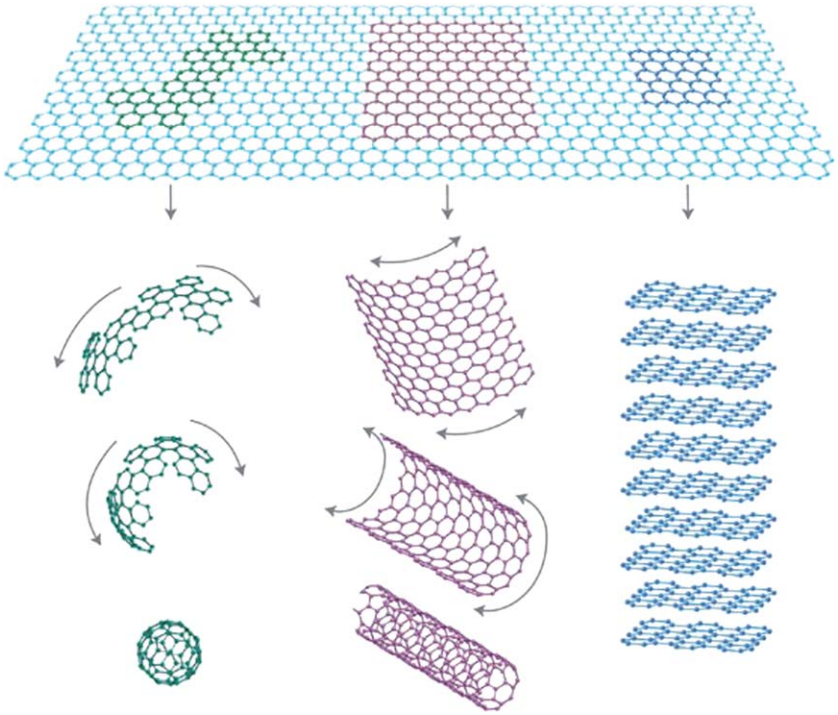

Fig. 1 Various carbon-based nanomaterials produced with a graphene sheet as a basic building block.[22] (Reprinted by permission from ref. 22, Geim and Novoselov, *Nat. Mater.*, 2007, **6**, 183; Copyright© Macmillan Publishers Ltd.)

not discussed, is the charge-overcompensation, in which mutually interacting polymeric species do not simply compensate the functionalities of each other, but rather over-compensate them.[31] In the case of LbL assembly onto colloidal particles, this behavior is commonly observed through the regular reversal of surface charges as measured by ζ-potential.

2.2. Multifaceted opportunity in LbL assembly: various parameters

As indicated above, the LbL technique is not only applicable to polyelectrolyte-based systems, but also to almost any type of charged species, including inorganic molecular clusters, nanoparticles,[32] nanotubes,[33] nanoplates,[34] micelles,[35,36] block copolymers,[37] polysaccharides,[38] polypeptides,[39] DNA,[40] and viruses.[41] These can be successfully incorporated as components to prepare LbL films. This translates into an exceptionally wide variety of structural characteristics which, in turn, create diverse functions. In addition, the ability to control their physical and chemical properties by controlling structural differences is widely believed to result in multifunctional films prepared by the LbL assembly.

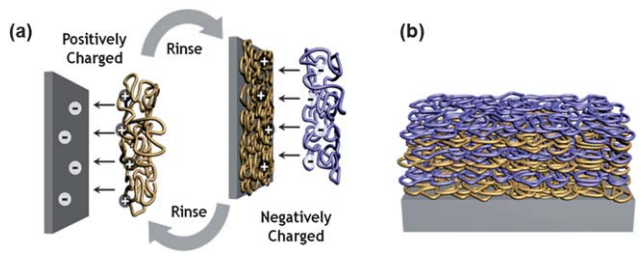

Fig. 2 (a) Schematic illustration of the layer-by-layer (LbL) assembled multilayer film deposition process based on electrostatic interaction. (b) A simplified multilayer film built up from a negatively charged substrate.

Although the electrostatic interactions are by far the most commonly adopted for the LbL assembly, other intermolecular interactions have been widely exploited in recent years, including hydrogen bonding, covalent bonding, charge transfer interactions, host-guest interactions, and even biological recognition motifs.[42,43] There also exist several reports of combining different intermolecular interactions to realize responsive LbL thin films. As a result, it would be highly desirable to investigate the effects of different molecular interactions to expand the utility of the LbL assembly.

During the LbL assembly, the film structure can be influenced by many parameters such as pH, ionic strength, and solute concentration of the solution. While materials with permanent charges are fully charged independent of pH, the weak polyelectrolytes bearing carboxylic acid or amine groups are highly sensitive to the pH of the external solution.[44,45] The conformation of weak polyelectrolytes can drastically change due to the change in charge density of the polymer electrolytes, while the conformation of strong polyelectrolytes is not altered. This unique responsive feature offers various possibilities that allow nanoscale control not only over the film thickness and roughness, but also over the internal structure with respect to solution pH.

With the progress of the LbL assembly, many different deposition methods have been developed with necessary instrumental developments, which add an additional source of versatility in the

LbL assembly. Beyond the most popular and traditional dipping method, spin-[46] and spray-assisted[47] LbL assemblies have recently been introduced as alternative LbL preparation methods (Fig. 3). These new assembly methods often result in well-defined multilayer films with a very short deposition period and, at the same time, a highly ordered internal structure that is often comparable but different from the conventional dipping-based LbL fabrication because the spin-assisted LbL deposition can induce not only interactions between polyelectrolytes but also strong centrifugal forces, viscous forces, and air-shear forces. Moreover, other distinguishing factors of this assembly process are low surface roughness due to low chain interpenetration of each layer, dense packing coverage, and time-efficient processing compared with the conventional dipping methods. Spray-assisted LbL deposition is also a powerful tool for preparing multilayer films not only on 2-dimensional but also on 3-dimensional substrates such as complex fabrics. In addition, the diversity of film properties could be realized by simply changing various parameters such as flow rate, sample to nozzle distance, and drainage time. Above all, the development of different deposition methods has significantly contributed to the advancement of the LbL community and its wide applications in many fields in terms of reducing the laborious processing time, enhancing the parameter control, and bringing this technique beyond the laboratory scale and more toward industrialized setup.

3. Functional multilayer films prepared by carbon materials

3.1. Functionalized carbon materials for LbL engineering

In comparison to conventional polyelectrolytes, the bulk carbon materials do not contain intrinsic surface charges and they also lack the suspension stability in aqueous media, which inevitably require additional steps in order to make them useful for LbL engineering. There are a number of approaches to achieve these objectives, including direct surface modification, surfactant-assisted dispersion, π–π stacking interactions with aromatic compounds, and functionalization with polymers.[48] Among the protocols mentioned above, the most common is the chemical oxidation of graphitic layers followed by organic modification with hydrophilic substances.[49] For example, the early work on the incorporation of fullerenes into LbL multilayer thin films was accomplished through the selective chemical modification of fullerenes with small organic functional groups such as porphyrins. Troisi and co-workers have reported on the functionalization of fullerenes and their potential use in optoelectronic devices.[50]

There have been several attempts to prepare multilayer LbL films of carbon nanomaterials, typically in combination with charged polyelectrolytes; however, the surface modification of carbon nanomaterials followed by the selective introduction of surface functional groups have yielded multilayer LbL films consisting exclusively of carbon materials. For example, Hammond and co-workers have reported on the facile functionalization of surfaces of multi-walled carbon nanotubes (MWNTs) *via* direct oxidation and selective surface modification to prepare charged MWNTs such as MWNT–COOH (MWNT–COO^-) and MWNT–NH_2 (MWNT–NH_3^+) (Fig. 4).[51] The direct functionalization on the surfaces of nanotubes allows the incorporation of negative charges both at the ends and along the backbone of nanotubes, preserving the colloidal stability in aqueous medium. In addition, the carboxylic acid functional groups on the nanotubes provide additional handles for further chemical modification with ethylenediamine in the presence of thionyl chloride, $SOCl_2$, yielding positively charged MWNT–NH_3^+. This simple chemical modification method offers virtually unlimited opportunities of expanding the material selection for the LbL deposition. X-Ray photoemission spectroscopy (XPS) elemental analysis supports the probing of surface functional groups on the modified MWNTs, as shown in Fig. 4. Moreover, ζ-potential measurements indicate the successful incorporation of functional groups responsible for the changes in ζ-potential with respect to the external pH condition. Specifically, carboxylic acid and amine groups grafted onto carbon nanotubes exhibit behaviors much like weak polyelectrolytes, such that the precise control on the degree of ionization of MWNTs is possible with a simple pH change. The multilayered MWNT films assembled with these oppositely charged MWNTs produce highly tunable films in terms of thickness, composition ratio, and porosity by controlling the degree of ionization of relevant MWNTs through the pH adjustment of assembly solutions. This ultimately influences the orientation of nanotubes within the film as well as film morphology.

This type of behavior is similarly observed in the case of common weak polyelectrolytes such as poly(allylamine hydrochloride) (PAH) and poly(acrylic acid) (PAA), which Choi and

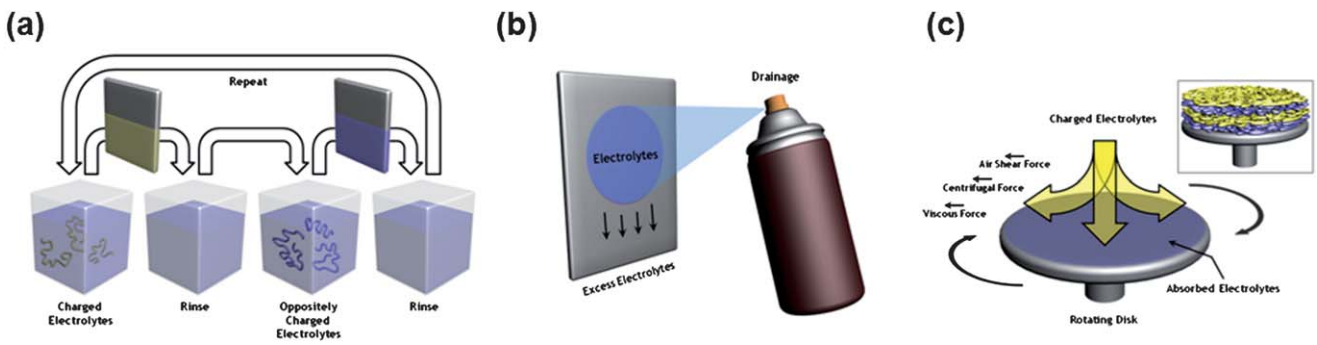

Fig. 3 (a) A schematic illustration of the multilayer film deposition process based on the dipping method. (b) An experimental setup for the multilayer film deposition by spraying. (c) A side view schematic depicting the build-up of multilayer assemblies by the consecutive spinning process of anionic and cationic polyelectrolytes.

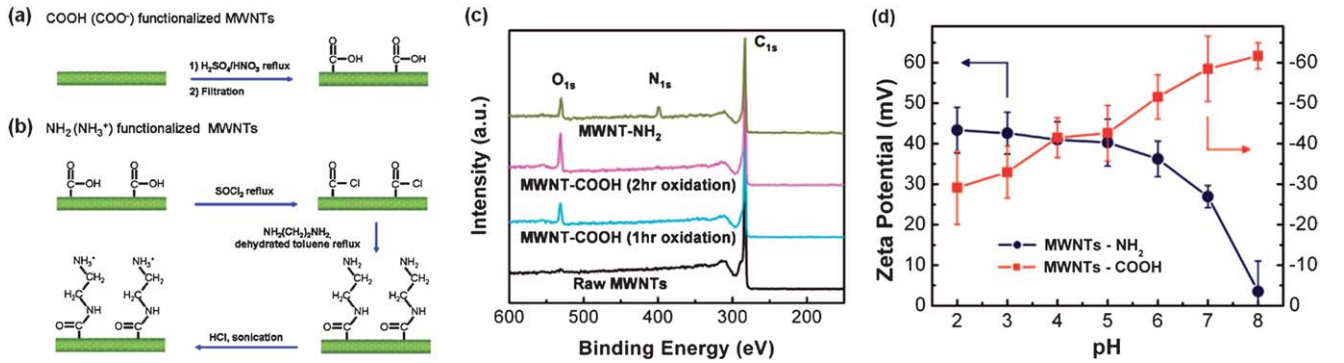

Fig. 4 Synthetic scheme of (a) COOH and (b) NH_2-functionalized MWNTs. (c) Wide survey scans of XPS spectra and (d) pH-dependent ζ-potential of functionalized (red) MWNT–COOH and (black) MWNT–NH_2. Reprinted with permission from ref. 51, Lee *et al.*, *J. Am. Chem. Soc.*, 2009, **131**, 671; Copyright© The American Chemical Society.

Rubner have previously demonstrated. The degree of ionization of weak polyelectrolytes is highly dependent on external pH condition, as briefly mentioned previously.[44] Similarly, the changes in the degree of ionization of surface functionalized carbon nanomaterials have a significant effect on the structure and properties of resulting multilayer LbL films. The carbon nanomaterials containing weak functional groups will thus offer many possibilities that allow nanoscale control over film thickness and roughness as well as internal structures by simply varying solution pH.

Identically, graphenes, which are promising novel nanomaterials with remarkable electrical, chemical and mechanical properties, could be modified by chemical functional groups. The most commonly used technique for the chemical oxidation of graphites to graphene oxides (GO) is by the exfoliation of natural graphite powders with various oxidants followed by sonication, first developed by Hummers, Brodies, and Stadudinger.[22,52,53] The solution-based route involves chemical oxidation of graphite to hydrophilic graphite oxide, which can be readily exfoliated as individual GO sheets by ultrasonication in water (Fig. 5). Graphene oxide, which is electrically insulating, can be converted back to conducting graphene by chemical reduction, for example, using hydrazine.

The chemically exfoliated graphene oxide sheets are well dispersed in aqueous solution due to charged functional groups such as carboxylic acid. These GOs can also be regarded as macromolecules with highly negative charges on their surfaces. Thus, they can be readily used to fabricate ultrathin films with polycations through the LbL deposition. Wallace and co-workers, for instance, have reported on the usage of negatively charged GO combined with positively charged polyelectrolytes, demonstrating the uniform coverage of graphene sheets on the surface of positive charged polyelectrolytes, poly(diallyldimethylammonium chloride).[54] Based on similar protocols presented for MWNTs, our group has recently reported the preparation of stable suspensions of GO that are highly stable and negatively charged over a wide range of pH conditions (GO–COO^-). Subsequent chemical modification with ethylenediamine in the presence of *N*-ethyl-*N*′-(3-dimethyl aminopropyl)carbodiimide methiodide (EDC) catalyst allows the introduction of amine groups (NH_2) on the surfaces of GO sheets, leading to positively charged stable GO suspensions (GO–NH_3^+) (Fig. 6). In order to recover the electrical properties of graphenes, the chemical reduction of GO suspensions was carried out by adding hydrazine in the presence of ammonia to prevent the aggregation of resulting reduced graphene oxide (rGO) nanosheets. As well demonstrated in ζ-potential measurements, the prepared GO and its corresponding rGO suspensions exhibit fairly good colloidal stability over a wide range of pH. It is also noted that these GO and rGO both display pH-dependent surface charges that are the typical characteristics of weak polyelectrolytes.[55,56]

3.2. Fabrication of electrical conducting multilayer films of carbon nanomaterials

The combination of unique electrical properties of carbon nanomaterials with the exceptional versatility of nanoscale organization of multilayer LbL films has opened up wide research opportunities. In particular, the transparent conducting electrodes made of carbon nanomaterials, typically single-walled

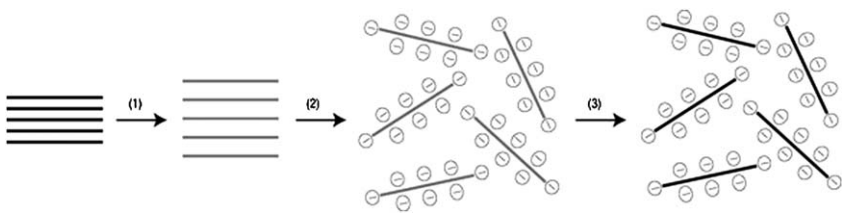

Fig. 5 Chemical exfoliation of graphites to graphene oxide nanosheets.[54] (1) Oxidation of graphites (black lines) to graphite oxide (light colored lines) with an increased interlayer spacing. (2) Exfoliation of graphite oxides in water by sonication to obtain GO colloids that are stabilized by electrostatic repulsion. (3) Controlled conversion of GO colloids to electrically conducting reduced graphene oxide colloids through deoxygenation with hydrazine. (Reprinted with permission from ref. 54, Li *et al.*, *Nat. Nanotechnol.*, 2008, **3**, 101; Copyright© Macmillan Publishers Ltd.)

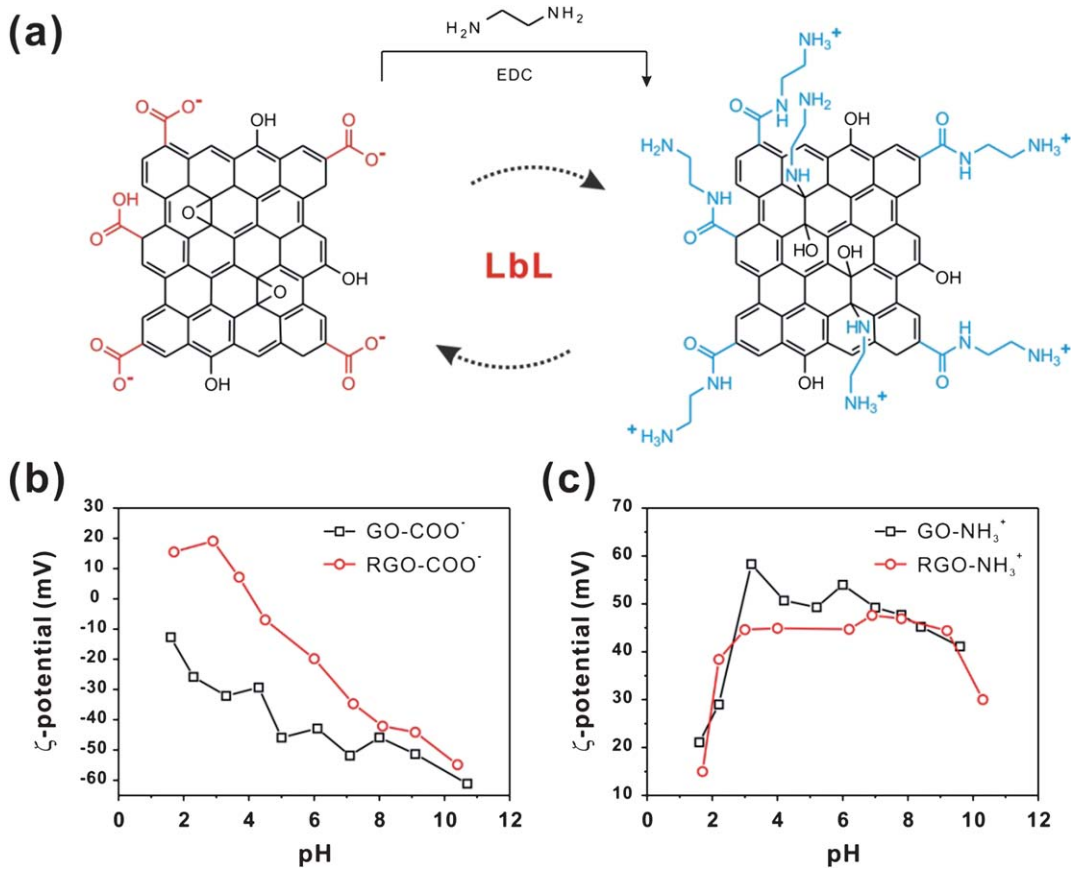

Fig. 6 (a) Synthetic scheme of oppositely charged GOs and (b and c) pH-dependent ζ-potentials of functionalized (b) GO–COO^- (black) and rGO–COO^- (red), (c) GO–NH_3^+ (black) and rGO–NH_3^+ (red).

carbon nanotubes (SWNTs) and graphenes, are now gaining much attention owing to their unique physical and electronic features. These conducting LbL films will prompt the creation of a new generation of electronics exemplified by bendable displays,[57] solar cells,[58] and large-area pressure detectors[59] as well as more exotic applications[60–63] that are currently impossible or hard to achieve with other materials.

As a seminal example, Kotov and Fendler *et al.* first reported the *in situ* reduction of a GO/polyelectrolyte composite film prepared by LbL assembly, forming a conductive composite.[64] Through the fine tuning of highly conductive SWNT *via* LbL assembly with polymers, Shim *et al.* reported the transparent conducting electrode with high conductivity of 86 ohm sq^{-1} at a moderate transparency of 85% combined with improved tensile modulus, strength and toughness of the film. Additionally, they observed that the molecularly thin polymeric binders between SWNT layers significantly improved mechanical stability, and clay capping *via* additional LbL assembly protected the transparent conducting electrode without sacrificing optical transparency as shown in Fig. 7.[65] These high electrical properties of SWNT LbL films were further demonstrated to be low cost, high efficiency polymeric thin film transistors by Xue *et al.* (Fig. 7).[66] The group has further suggested that these micro-patterned electronic devices could be fabricated on a highly flexible substrate by LbL assembly.[67]

In contrast to conventional application of SWNT in the transparent electrode, we have integrated GO with MWNT *via* the LbL approach to fabricate the hybrid transparent conducting electrode.[56] This method affords a hybrid multilayer of $(MWNT/GO)_n$ with well-controlled optical and electrical properties. The hybrid multilayer exhibits a significant increase in electronic conductivity after thermal treatment, yielding a transparent and conductive thin film with a sheet resistance of 8 kohm sq^{-1} and a transparency of 82%. The flexibility of the hybrid $(MWNT/rGO)_n$ multilayer coated on the PET substrate was further demonstrated by comparison with commercial ITO-coated PET. Though the absolute sheet resistance values are higher than that of the commercial product, we found that our hybrid film maintains its electrical conducting properties under excessively bending conditions and retained the initial values over 100 cycles (Fig. 8). In contrast, the commercial ITO-coated PET loses its conductivity after a few bending cycles due to surface cracks originating from the rigid inorganic nanostructures.

In an extension to this study, we have also recently demonstrated that the assembled reduced graphene oxide based multilayer of $(rGO/rGO)_n$ is a transparent conducting electrode possessing high electrical conductivity with varying transparency.[68] The sheet resistance decreases linearly with increasing number of bilayers with precise control over the thickness of each bilayer down to *ca.* 0.72 nm—close to the theoretical values of graphitic layers. In the present study, the lowest sheet resistance is 2.5 kohm sq^{-1} at 75% transmittance. The sheet resistance and transmittance can be easily changed in conjunction with the number of bilayers which is strongly related to the thickness of

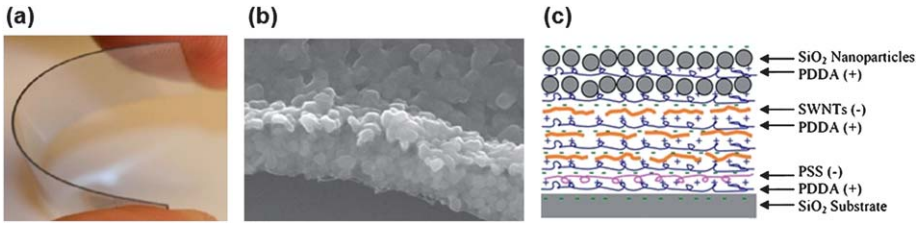

Fig. 7 (a) Photo images of bending of the SWNT LbL coating on the PS substrate. (b) Cross-sectional SEM image of the assembled SWNT/SiO_2 layers which consists of a SWNT multilayer, a SiO_2 multilayer, and an Al layer. The SWNTs and SiO_2 nanoparticles are closely packed in the thin film. (c) Structure of LbL self-assembled SWNT semiconducting layer and SiO_2 nanoparticle dielectric layer. (Reprinted with permission from ref. 65 and 66, Shim *et al.*, *ACS Nano*, 2010, **4**, 3725; Copyright© The American Chemical Society, Xue *et al.*, *Appl. Phys. Lett.*, 2006, **89**, 163512; Copyright© American Institute of Physics.)

the multilayers. This means that we can precisely control the thickness, sheet resistance, and transmittance of the multilayers by fully taking advantage of nanoscale engineering of the LbL assembly (Fig. 9). Furthermore, we show that the rGO multilayers can be used as transparent electrodes for organic light-emitting diode (OLED) devices. The current density–voltage–luminance (*J–V–L*) characteristics of the device fabricated on the rGO multilayer coated substrate are shown in Fig. 9. In comparison with the ITO electrode device which shows a maximum luminance of ~7800 cd m^{-2} at 6 V, the rGO multilayer electrode device shows relatively low luminance of ~70 cd m^{-2} at 18 V. However, it is of note that the luminous efficiency of the device with the rGO electrode is ~0.10 cd A^{-1} which is comparable to that of the ITO electrode, ~0.38 cd A^{-1}.

Another interesting example is reported by Yu *et al.* who used the SWNT/PDDA multilayer composite with 2.5 kohm sq^{-1} at 86.5% transmittance.[69] They further formed the similar LbL coating as a transparent surface electrode on a PVDF actuator for an audio speaker.[70] In summary, the transparent conducting electrode of carbon nanomaterials will provide direct commercialization opportunities utilizing precise nanoscale organization of LbL assembly together with the interesting electronic properties of carbon nanomaterials.

3.3. Multilayer films for electrochemical applications

Due to the combination of the unique merits of LbL assemblies, such as ultrathin and highly controlled internal structures and porosity, and the high conductivity of carbon nanomaterials, many electrochemical devices such as batteries, supercapacitors, and proton exchange membranes for fuel cells were constructed using LbL assembled carbon nanomaterials as highly conductive and chemically durable electrodes.[71–75]

As mentioned above, Hammond and Shao-Horn reported morphologically tunable all MWNT thin films created by LbL deposition.[51] Negatively and positively charged MWNTs were prepared by surface functionalization, allowing the incorporation of MWNTs into highly tunable thin films *via* the LbL technique. The conformal and uniform MWNT multilayer films are generated with highly interpenetrated and porous structures. Since the MWNTs have intrinsically high electrical conductivity and higher surface area, these porous network structures can work as fast electronic and ionic conducting channels, providing the basis for the design of an ideal matrix structure for energy conversion as well as energy storage devices. The group has further extended the approach in creating an electrode with high capacitance anode materials for the Li-ion battery.[33] The porosity as well as the intrinsic conductivity of the graphene structures on the surface of MWNTs provides a pathway for the electrical current as shown in Fig. 10. Multilayered MWNT electrodes have a high rate capability because of the stored energy on the surfaces of MWNTs. The current at 3 V was found to increase linearly with scan rates from cyclic voltammetry, indicating a surface-redox limited process at a given thickness (Fig. 10). This agrees well with the proposed mechanism of redox active functional groups on MWNT surfaces. In addition, LbL-MWNT electrodes with 0.3 μm thickness exhibit the gravimetric capacity of ~200 mA h g^{-1} at low rates such as 0.4 A g^{-1}, which is in agreement with the estimated capacity of

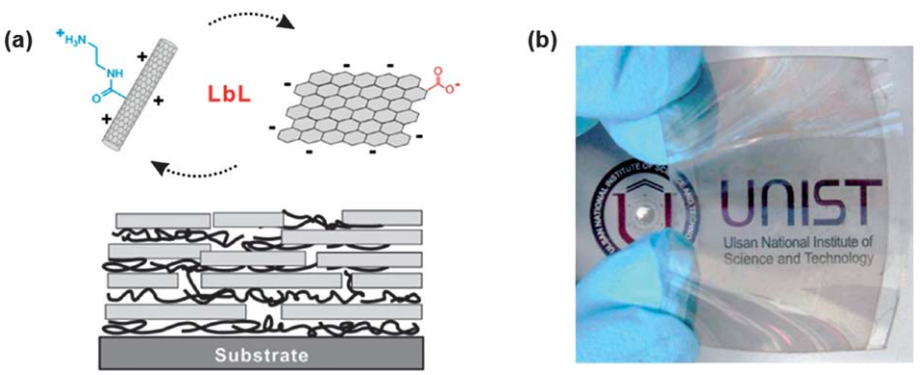

Fig. 8 (a) Schematic representation of hybrid LbL multilayer of MWNTs and rGO and (b) image of $(MWNT/rGO)_{25}$ hybrid thin film on a PET substrate after mild thermal treatment. (Reprinted with permission from ref. 56, Hong *et al.*, *ACS Nano*, 2010, **4**, 3861; Copyright© The American Chemical Society.)

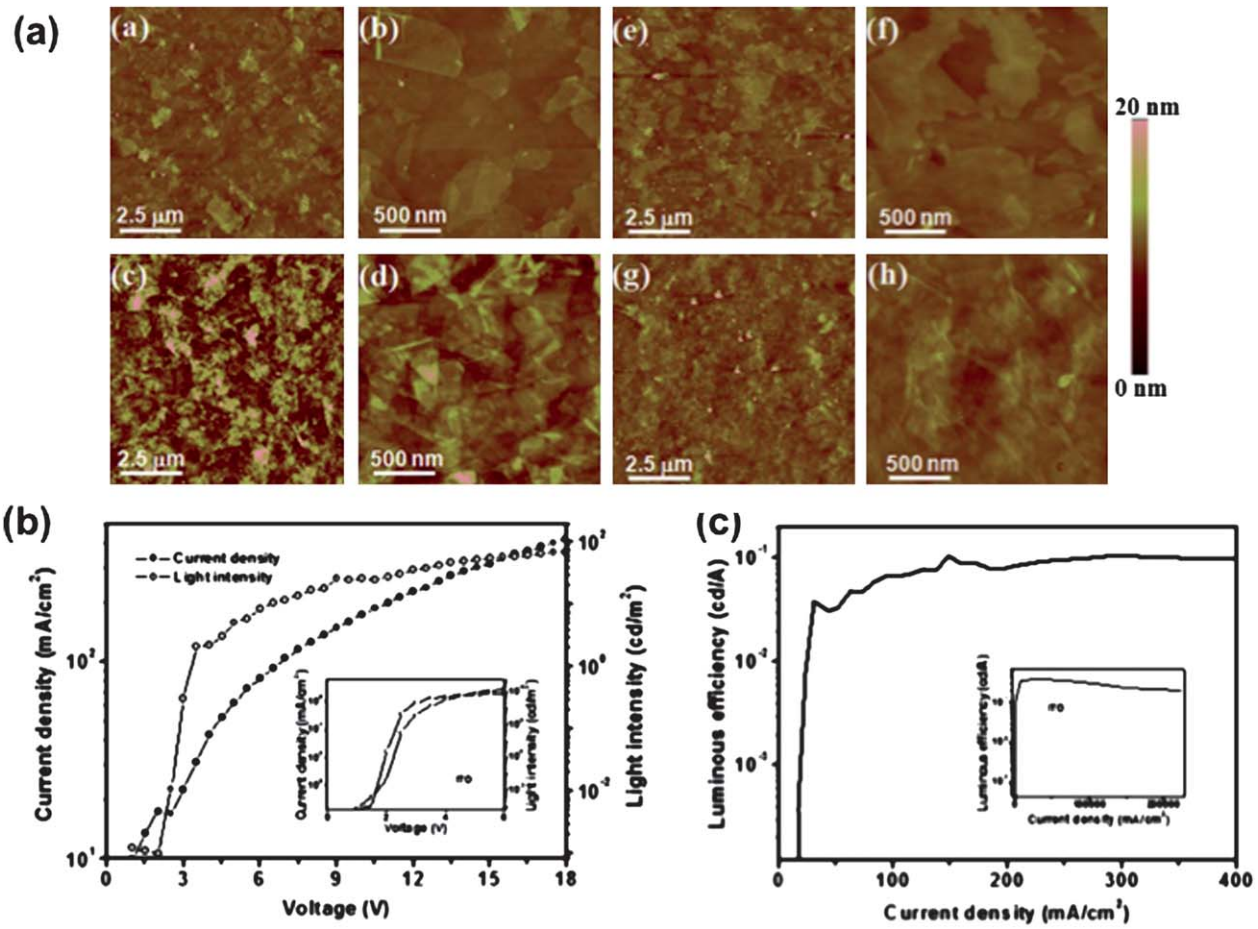

Fig. 9 (a) AFM images of rGO multilayers on quartz substrates before (a–d) and after (e–h) annealing in H_2 atmosphere at 1000 °C for $n = 2$ bilayers (top panels; a, b, e, and f) and 10 bilayers (bottom panels; c, d, g, and h). Scale bar is 2.5 mm and 500 nm as indicated, respectively. (b) Current density–voltage–luminance (J–V–L) characteristic of the OLED device using the rGO electrode with 3 kohm sq^{-1}. The inset is the electroluminescence property of the device fabricated with the ITO electrode. (c) Luminous efficiency of the device with the rGO electrode. The inset is luminous efficiency of the device fabricated with the ITO electrode.

LbL-MWNT electrodes based on the proposed Faradaic reaction between Li and surface oxygen. Half of the gravimetric capacity (100 mA h g^{-1}) was retained at exceptionally high discharge rates of 180 A g^{-1}.

Moreover, successive experimental reports confirmed that LbL assembly of SWNTs indeed exhibits exceptional applications in fuel cells. The multilayered Nafion and Pt catalysts modified SWNT showed unusual fuel cell performances in a fuel cell polymer electrolyte membrane, which has nanoscale optimized electron/proton movements, simple and low cost production, and efficient utilization of Pt catalysts. Moreover the mechanical strength, high electrical and thermal conductivities, and stable chemical durability are the result of SWNT based membranes (Fig. 11).[76] For the 400 bilayered [poly(ethyleneimine)(PEI)/(Pt/SWNT + Nafion)] catalysts, the peak power densities were as high as 195 $mWcm^{-2}$, which is much higher than that of previously reported LbL films.[25] This LbL approach is further adapted as a blending technique between proton exchange Nafion and SWNTs to control layers for improving proton conduction efficiency at a high operating temperature.

Interestingly, uses of carbon nanotubes are also developed for biofuel cell applications by generation of electrical potential by stable enzyme immobilization.[77] For example, Zhou *et al.* showed a biofuel cell with high power density prepared by mesoporous carbon materials by taking advantage of the conductivity and large surface area of carbon nanotubes for depositing the enzymes.[78] Recently, polyelectrolyte wrapped MWNTs are also used to dope polyaniline (PANI) and shift its electroactivity to a neutral environment. The nanoscale assembly by LbL assembly presents new possibilities for tackling the nanostructured process of MWNT/PANI composites and presents a potential for electrochemical device production.[79] In summary, the multilayered nanotube-based multilayer films are a promising design for integration of a micro-device for electrochemical applications. To meet the demands of these applications, multilayer film prepared by LbL assembly will provide broad opportunities to organize functional objects with MWNTs to control the structure of the build materials at a nanoscale with a high degree of accuracy.

3.4. Multilayer films for sensor applications

A great deal of carbon-based nanocomposites fabricated by LbL assembly techniques were applied to physical, chemical, and biological sensors by utilizing either (1) electrical property

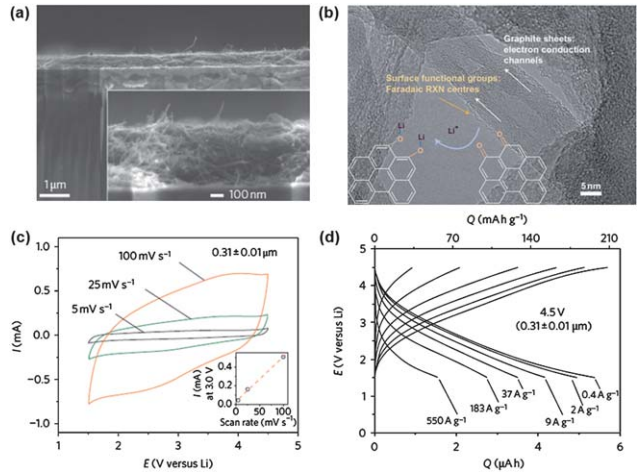

Fig. 10 (a) SEM cross-sectional image of an LbL-MWNT electrode on an ITO-coated glass slide after heat treatments. A higher-magnification image is shown in the inset, revealing that MWNTs are entangled in the direction perpendicular to the electrode surface. (b) Schematic of the energy storage mechanism of LbL-MWNT electrodes: Faradaic reactions between surface oxygen functional species (orange arrows) and Li schematically illustrated on an HRTEM image of the LbL-MWNT electrodes. (c) Cyclic voltammogram data for a 0.3 μm LbL-MWNT electrode over a range of scan rates. The current at ~3 V *versus* scan rate is shown in the inset (d) charge and discharge profiles of an electrode of 0.3 μm obtained over a wide range of gravimetric current densities between 1.5 and 4.5 V *versus* Li. (Reprinted with permission from ref. 33, Lee *et al.*, *Nat. Nanotechnol.*, 2010, **5**, 531; Copyright© Macmillan Publishers Ltd.)

changes of nanotubes or graphenes by chemical species, (2) electrochemical responses of the counterpart of CNTs, or (3) structural deformation induced electrical resistance changes of a composite. Due to its unique geometry and electrical and mechanical properties, CNTs are leading these frontiers over various other carbon nanomaterials.

Kotov and co-workers have reported the production of smart electronic yarns by a simple process of transforming cotton threads into intelligent e-textiles using a polyelectrolyte-based coating with SWNT.[80] They further demonstrate that CNT-cotton threads can be used to detect albumin, the key protein of blood, with high sensitivity and selectivity, which present an important application of wearable fabrics for biomonitoring (Fig. 12). Typical examples of monitoring physical and chemical states by carbon nanotube LbL composites are demonstrated by Loh *et al.*[81] In an attempt to control the macro-scale sensitivity of CNT-polyelectrolyte thin-film electrical changes to strain or pH stimuli, fabrication parameters (*i.e.* CNT and polyelectrolyte concentrations) and the type of CNT (*i.e.* unpurified SWNTs, purified SWNTs, and purified double-walled carbon nanotubes (DWNTs)) are experimentally varied to quantify changes in the performance characteristics of CNT-poly(sodium 4-styrenesulfonate) (PSS) with strain and pH sensors. They reported that a strain sensor by tailored piezoresistive response and a pH sensing strip sensitive enough to monitor environment changes caused by corrosion of metal structures were constructed by SWNT/poly(vinyl alcohol) (PVA) and SWNT/PANI LbL composites, respectively.

Detection targets of carbon material based LbL composites include various important biological materials such as DNA, glucose, dopamine, and toxic materials. These targets are often detected by amperometric measurements of CNT-based LbL nanocomposites utilizing the combinations of electrocatalytic activities, electrochemical sensitivities of CNTs, and various material immobilizations given by versatile selections of LbL assembly. Recently, Kim and Hammond developed a multilayer film prepared by MWNT *via* the pattern transfer technique (Fig. 13). This patterned MWNT multilayer was precisely tunable with the thickness and exhibits a capacitor behavior that increases with growing film thickness. By taking full advantage of patterned electrodes with high surface functionality within an MWNT network, potential patterned MWNT electrodes are demonstrated as sensitive glucose biosensors.[82]

The LbL assembly also offered the development of strong antimicrobial coatings by multifunctional biomimetic material comprised of SWNT, DNA, and lysozyme (LSZ). By successful alternative deposition of LSZ–SWNT/DNA–SWNT, the multilayer films ending in LSZ–SWNT layers exhibit great antimicrobial activity compared to the initial dispersion (Fig. 14). Moreover, no leaching of the enzyme was observed over 60 days and this non-leaching coating exhibits robust mechanical properties and long-term protection against bacterial colonization.[83]

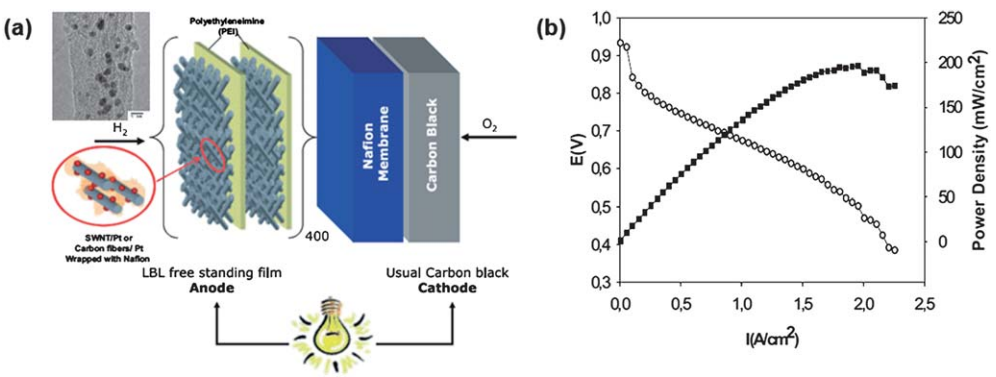

Fig. 11 (a) Overall schematic illustration of preparation of the LbL films (inset: TEM images of Pt/SWNT). (b) Polarization (○) and power density (●) curves of fuel cells with LbL film anodes: $[PEI/(Pt/SWNT + Nafion)]_{400}$. The fuel cell temperature was 80 °C. H_2 and O_2 flows on the fuel cell saturators were set at 100 sccm flow rates, 100% relative humidity, and 90 °C temperature. (Reprinted with permission from ref. 76, Michel *et al.*, *Adv. Mater.*, 2007, **19**, 3859; Copyright© Wiley.)

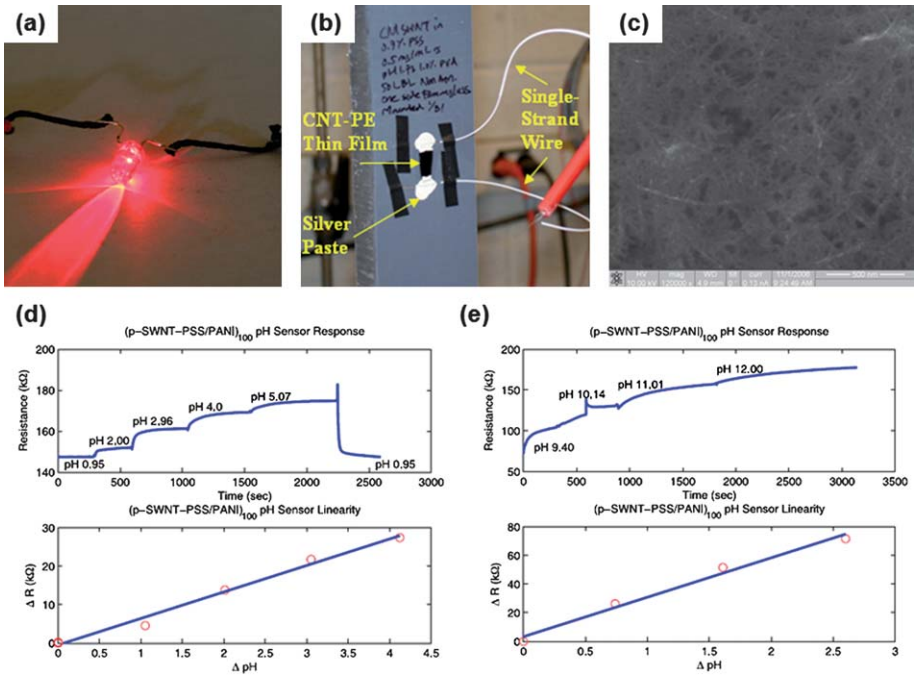

Fig. 12 (a) Photographs of SWNT-cotton yarn demonstrating LED emission with the current passing through the yarn. (b) SWNT–PSS/PVA strain sensor on glass epoxy-bonded to a PVC specimen. (c) SEM image of $(SWNT–PSS/PVA)_{50}$ thin film. (d), (e) Top, $(p\text{-}SWNT–PSS/PANI)_{100}$ (d) acidic (pH 0.95–5.07), (e) alkaline (pH 9.40–12.00) solution pH sensing response; bottom, normalized change of resistance as a function of pH, indicating linearity of pH sensor (d) (sensitivity, $S_P = 4.56$ kohm cm^{-2} pH^{-1}), (e) (sensitivity, $S_P = 20.66$ kohm cm^{-2} pH^{-1}). (Reprinted with permission from ref. 80 and 81, Shim *et al.*, *Nano Lett.*, 2008, **8**, 4151; Copyright© The American Chemical Society, Loh *et al.*, *Smart Mater. Struct.*, 2007, **16**, 429; Copyright© IOP Publishing.)

Furthermore, in respect to sensing applications of MWNT multilayers, one of the additional interests is once again in a potential for enhanced stability due to the multilayered structures of MWNTs. With its controllable resistance of MWNTs and superior mechanical properties, a novel flexible H_2 gas sensing membrane was successfully fabricated by LbL assembly of MWNTs and Pd on a modified PET substrate (Fig. 14). The Pd nanoparticles decorated with MWNTs are ideal materials in the fabrication of a high performance, flexible, highly responsive and reliable H_2 sensor.[84]

The carbon-based nanomaterial films prepared by LbL assembly with nanoscale complexation serve as an emerging platform for the preparation of both energy storage electrodes and sensing applications. LbL assembled multilayer structures offer interesting possibilities; highly controlled internal structures yield high surface area, high porosity, enhanced mechanical properties and additional functionality from counter assembled functions that enabled multi-properties while maintaining a simple aqueous based process. As a summary, we have provided Table 1 consisting of previous reports on the preparation of carbon-based multilayers.

4. Carbon-based hollow capsules by layer-by-Layer

4.1. Hollow capsules based on LbL assembly

As we have discussed in previous sections, the LbL approach has the versatility to be assembled on various substrates, particularly on three-dimensional colloidal particles. The removal of the colloid templates following the LbL multilayer deposition can give rise to hollow capsules. The capsule structure can have a variety of applications, including the encapsulation and sensing,[103] controlled release of drugs or genes,[104,105] and the electrocatalytic reactions for energy devices.[106]

Fig. 15 shows a schematic illustration of the typical procedure for fabrication of the capsule structure. With colloidal particles being employed as templates, we deposit LbL multilayer films onto the outer surface of the colloidal particles typically based on intermolecular interactions such as electrostatic interactions,[8] hydrogen bonding,[107] hydrophobic interactions,[108] covalent bonding,[109] and complementary base paring,[110] and so forth.

In order to remove the core template materials, either the swelling of the core polymer by a relevant solvent or the thermal treatment (calcinations) of the organic templates is typically used. This fabrication method allows the excellent control over the properties of hollow shells, such as size, composition, thickness, and functionality, by varying the size and the shape of the template colloids as well as the film constituents.

For core materials to be removed to yield hollow shells, solid spheres of polystyrene (PS), melamine formaldehyde (MF), or silica particles have widely been used for various LbL multilayer films incorporated into the hollow capsules. The use of PS colloids requires solvents such as tetrahydrofuran (THF) to effectively remove the PS colloids to form hollow capsules, while MF colloids are chemically decomposed under acidic conditions.[111] Although the decomposition of silica template particles typically involves the use of HF, ammonium-fluoride-buffered HF solution at mild pH can be used in the presence of biological

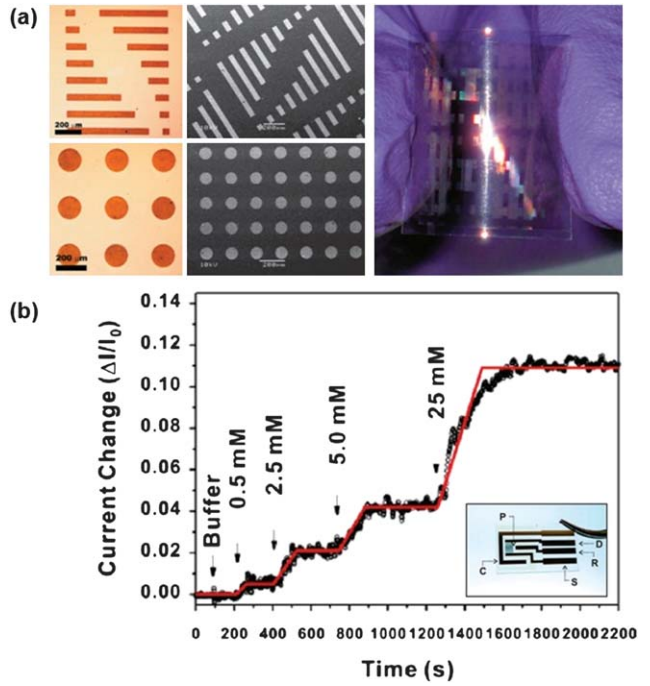

Fig. 13 (a) Representative (left) optical microscope and (middle) SEM images of patterned MWNT multilayer film on a silicon wafer, (right) photograph of MWNT pattern transferred on a flexible ITO-coated PET film. (b) Real-time response of the sensor upon a serial addition of 0.5–25.0 mM glucose (the arrow indicates the addition of analyte solutions) (inset: photograph of the patterned enzyme-MWNT film on interdigitated microelectrode array—the patterned MWNT film (P), source (S), drain (D), reference (R), and counter (C) electrodes are individually labeled.) (Reprinted with permission from ref. 82, Kim *et al.*, *Chem Mater.*, 2010, **22**, 4791; Copyright© The American Chemical Society.)

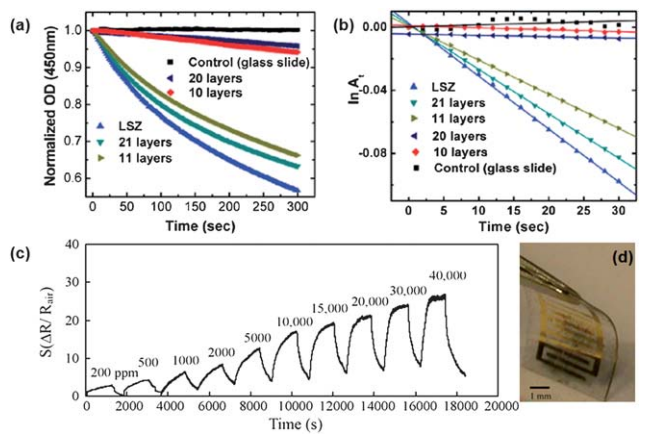

Fig. 14 (a) Effect of different layers of LBL coating against *M. lysodeikticus* in turbidimetric assay. (b) Rate of *M. lysodeikticus* lysis reaction (regression line is fit to the linear portion of experimental data in (a) using first-order rate kinetics). (c) Response curve of flexible MWNT–Pd film H_2 sensor as function of time (s) for various concentrations of H_2 gas. (d) Photograph of bent flexible H_2 gas sensor based on MWNT–Pd film, assembled on PET substrate. (Reprinted with permission from, ref. 83 and 84 Nepal *et al.*, *Nano Lett.*, 2008, **8**, 1896; Copyright© The American Chemical Society, Su *et al.*, *Actuat. B*, 2010, **145**, 521; Copyright© Elsevier.)

materials without significant damage to its bioactivity.[112] Gold nanoparticles,[113] emulsion droplets,[114] and gas bubbles[115] have also been used as sacrificial colloidal templates.

The vast majority of capsules prepared from these colloidal templates have been assembled by the alternate deposition of positively and negatively charged chains or particles, where the long-ranged Coulombic interactions govern the multilayer buildup. Such hollow capsules retain the spherical shape of the original particle templates when dispersed in solution. However, when those hollow capsules are air-dried onto a substrate, they show a collapsed structure that resembles deflated balloons. On the other hand, inorganic hollow capsules possess other advantages such as superior mechanical and thermal stability. These can be prepared with either preformed nanoparticle building blocks or inorganic molecular precursors.

4.2. Hollow capsules of carbon nanomaterials

Carbon-based materials, such as fullerenes (0D),[116,117] carbon nanotubes (CNT) (1D),[118–120] and graphenes (2D),[121–123] have been extensively studied because of their distinct electrical and mechanical properties. Many researchers have developed recently and have keen interests in carbon-based hollow capsules, which have potential applications for drug delivery due to their inherent biocompatibility, and for sensor or electrochemical devices owing to unique electrical properties of the carbon-based nanoscale objects. As mentioned in the previous section, the carbon-based materials could also have positive or negative charges on their surfaces through functionalization with amines or carboxylic acid groups. Various preparation methods to obtain hollow capsules have been reported, based on the LbL assembly of charged carbon materials on various spherical templates such as melamine (MF), polystyrene (PS), and so forth. The previous reports on the preparation of carbon-based hollow capsules are summarized in Table 2.

There have been several attempts to prepare hollow capsules by the LbL deposition of carbon nanotubes, typically in combination with polyelectrolyte chains on colloidal templates followed by the removal of the core templates.[127,130] The starting colloidal templates (PS or SiO_2) containing negative or positive charges on their surfaces were coated with an oppositely charged polyelectrolyte in order to obtain a uniformly charged layer for additional deposition. Charged CNTs can be prepared by chemical oxidation methods using sulfuric and nitric acids to form oxygen containing groups, such as carboxylic groups, at both tips and sidewalls on CNTs. These functional groups are responsible for the presence of negative charges which afford a stable dispersion of individual CNTs in water as well as to assemble on positively charged surfaces. M. Correa-Duarte and co-workers reported polyelectrolyte/CNT hollow capsules, derived from the LbL deposition on colloidal templates followed by dissolution in a good solvent for the templates to remove the core templates. As shown in Fig. 16a, the deposition of CNTs on colloidal templates is successfully demonstrated; however, after removing the core templates, the hollow shells consisting of polyelectrolyte/CNT typically collapse due to the relatively weak mechanical strength as shown in Fig. 16b. Fig. 16c shows a TEM image of MWNT/PAH/PSS hollow capsules after the core MF templates are removed. In this case, C. Gao and co-workers used

Table 1 Carbon-based multilayered films prepared by the LbL assembly and their applications

Carbon materials	Layered materials	Applications	References
MWNT	PEI/MWNT/PAA	Biomedical and structural materials	N. A. Kotov, M. Giersig *et al.*, *Nano Lett.* (2004)[85]
	MWNT/PDDA, MWNT/Au	Bioelectronic devices	L. Mao *et al.*, *Carbon* (2006)[86]
	MWNT/Au	Biosensors	Y. Zhang *et al.*, *Electrochim. Acta* (2008)[87]
	PANI/MWNT/PSS	Electrochemical devices	Y. Xian *et al.*, *Carbon* (2010)[88]
	PEI/MWNT	Anode for fuel cell	H.-Z. Zhao *et al.*, *Electrochim. Acta* (2010)[74]
	MWNT/PAH/Pd	Gas sensors	P. G. Su *et al.*, *Sens. Actuators, B*, (2010)[84]
	MWNT/MnO_2	Electrochemical capacitors	P. T. Hammond, Y. Shao-Horn *et al.*, *ACS Nano* (2010)[18]
	MWNT/MWNT	Glucose biosensor, high-power lithium batteries	P. T. Hammond *et al.*, Chem. Mater. (2010),[82] P. T. Hammond, Y. Shao-Horn *et al.*, *Nat. Nanotechnol.* (2010)[33]
	PANI/MWNT	Electrochemistry supercapacitors	Y. Xian *et al.*, Carbon (2010),[88] G.-C. Wang *et al.*, *Electrochim. Acta* (2011)[89]
SWNT	PDDA/PSS/SWNT–pyrene/ polythiophene	Photodevices	D. M. Guldi, L. Schenetti, M. Prato *et al.*, *J. Am. Chem. Soc.* (2005)[90]
	PVP-Os/glucose oxidize-SWNT	Biosensors	D. W. Schmidtke *et al.*, *Langmuir* (2006)[91]
	PEI/SWNT/PLO	Substratums for neural stem cells	N. A. Kotov *et al.*, *Nano Lett.* (2007)[60]
	SWNT/PVA and SWNT/PANI	Biosensors	N. A. Kotov *et al.*, *Smart Mater. Struct.* (2007)[81]
	Lysozyme–SWNT/DNA–SWNT	Antimicrobial coatings	D. Nepal *et al. Nano Lett.* (2008)[83]
	SWNT/PVA	Mechanical support	N. A. Kotov *et al.*, *ACS Nano* (2009)[92]
	ITO/PDDA/PSS/SWNT–pyrene	Solar cell	M. Prato, L. Schenetti, D.-M. Guldi *et al.*, *J. Mater. Chem.* (2009)[93]
	PVA/SWNT/PSS(SDS)	Flexible transparent conductors	N. A. Kotov *et al.*, *ACS Nano* (2010)[65]
Carbon black	CB/Al_2O_3	Energy storage devices	D. Lee *et al.*, *Langmuir* (2010)[94]
Mixed	MWNT/rGO	Transparent conducting electrode	H. Shin, B. Kim *et al.*, *ACS Nano* (2010)[56]
	MWNT/GO(rGO)	Electrochemical capacitors	Y. Shao-Horn *et al.*, *Carbon* (2011)[95]
Graphene	PAA/GO	Conducting film	J. Wu *et al.*, *Langmuir* (2008)[61]
	rGO/Au	Biosensors	H. -T. Jung *et al.*, *Chem. Commun.* (2009)[62]
	PEI/TiO_2/GO	Photo-conversion	K. P. Loh *et al.*, *Adv. Funct. Mater.* (2009)[96]
	PMMA/GO, PVA/GO	Structural support	S. T. Nguyen, L. C. Brinson *et al.*, *Adv. Funct. Mater.* (2010)[97]
	rGO/Pd	Hydrogen sensors	U. Lange *et al.*, *Electrochim. Acta* (2010)[98]
	PEI/rGO	Supercapacitors	V. Meunier, P. M. Ajayan *et al.*, *Nano Lett.* (2011)[63]
	rGO–IL/PSS	Gas sensors	Q. Ji, I. Honma, K. Ariga *et al.*, *J. Am. Chem. Soc.* (2010)[99]
	PAH/PSS/GO	Mechanical support	V. V. Tsukruk *et al.*, *ACS Nano* (2010)[100]
	rGO	Conducting film for OLED	B. Kim, H. Shin *et al.*, *J. Mater. Chem.* (2011)[68]
	PDDA/PSS/PAH/GO	Conducting film	M. Park *et al.*, *Appl. Surf. Sci.* (2011)[101]
	PDDA/PSS/rGO/MnO_2	Supercapacitors	J. Wang, S. Yang *et al.*, *J. Mater. Chem.* (2011)[102]

PAH as a positive charged electrolyte because MWNTs have negative charges. To enhance the mechanical properties of the shell phase, there have also been attempts to incorporate inorganic components into the CNT/PDDA hollow capsules by Y. Lu and Z. Yang and co-workers as demonstrated in Fig. 16d.

4.3. Graphene hollow capsules

One alternative candidate to impart mechanical strength on the hollow spheres would be to use reduced graphene oxide nanosheets, as we have recently reported. With similar approaches taken for CNTs, graphene sheets can also be employed as

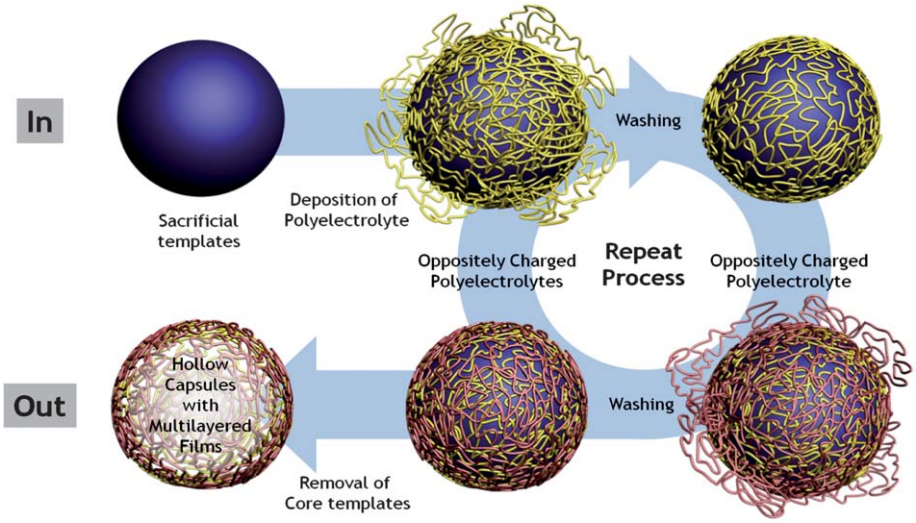

Fig. 15 A schematic illustration of preparing hollow capsules containing polyelectrolyte multilayer films by the layer-by-layer assembly on sacrificial colloidal templates.

a component for the layer-by-layer deposition to build graphene-based hollow capsules. By the Hummer's method discussed in the previous section, we could produce hydrophilic, negatively charged graphene oxide sheets with high dispersion capability due to the formation of oxygen containing species such as carboxylic acids, epoxide, and hydroxyl groups on the surfaces of graphene sheets. Following sonication for the exfoliation of graphite oxide sheets, chemical functional groups are introduced onto the surfaces of graphene sheets, particularly carboxylic acids (COOH), to create the negatively charged GO sheets (GO–COO^-). Positively charged GO sheets are subsequently prepared by introducing amine groups (NH_2) on the surface of negatively charged GO sheets by the EDC-mediated reaction. Chemical reduction was carried out typically by adding hydrazine to afford rGO–COO^- and rGO–NH_3^+.

The hollow graphene capsules were prepared based on the electrostatic interactions by the repetitive depositions of rGO–NH_3^+ and rGO–COO^- on PS colloid templates to realize multilayered thin films in the architecture of (rGO–NH_3^+/rGO–COO^-)$_n$. After the LbL deposition with graphene sheets, as demonstrated with previous reports using sacrificial templates to create hollow nanostructures, hollow capsules consisting of rGO sheet-paired multilayers were recovered by removing PS colloid templates by dissolving in THF. Fig. 17a shows the schematic illustration of the graphene hollow capsule process. On the basis of the stable growth of (rGO–NH_3^+/rGO–COO^-)$_n$ multilayers on colloidal substrates, the morphology of PS colloids encapsulated with rGO sheets have been investigated with SEM and TEM. We found that the graphene sheets are uniformly coated on PS colloidal templates, yielding fairly smooth surface morphology. After removing the PS colloidal templates, the (rGO–NH_3^+/rGO–COO^-)$_n$ multilayers lead to hollow capsules with some wrinkles on their surfaces (Fig. 17c). After the core templates are removed, it is noted that the hollow capsules maintain their spherical shape without any supporting components, which has not been observed in the hollow capsules based on the combination of CNTs and polyelectrolytes. Graphene hollow capsules preserve their spherical shape even with a low deposition number (>3 bilayers) due to stronger collective mechanical strength of graphene sheets when compared with a combination of CNTs and polyelectrolytes, particularly for three-dimensional structures.

4.4. Graphene-functional nanoobject hybrid hollow capsules

In addition, the shell phase of graphene capsules has been modified with various functional species such as poly(ethylene glycol), lipids, antibodies, and functional nanoparticles by taking advantage of the key feature of the LbL deposition: insertion of functional nanoscale objects at any desired position during the

Table 2 Carbon-based hollow capsules prepared by the LbL assembly on colloidal templates

Template materials	Layered materials	Method of template removal	References
PS colloids	Graphene oxides	Dissolved in THF	K. Char, B. Kim *et al.*, *J. Phys. Chem. Lett.* (2010)[14]
	PDDA/CNT/SiO_2	Dissolved in DMF	Z. Yang *et al.*, *Chem. Comm.* (2006)[124]
	PDDA/PSS/PAH/MWNT	Dissolved in CH_3Cl	M. Correa-Duarte *et al.*, *Small* (2008)[125]
Melamine formaldehyde colloids	PSS/PAH/MWNT	Dissolved in HCl	C. Gao *et al.*, *Macromol. Rapid. Commun.* (2004)[126]
	PDDA/PSS/CNT	Dissolved in HCl	M. Correa-Duarte *et al.*, *Chem. Mater.* (2005)[127]
Silica colloids	SWCNT	Dissolved in HF	M. Sano *et al.*, *Nano Lett.* (2002)[128]
	Curdlans–SWNT complexes	Dissolved in HF	S. Shinkai *et al.*, *Langmuir* (2008)[129]
Poly(methacrylic acid) (PMAA) colloids	PDDA/MWNT	Calcination above 400 °C	J. Shi *et al.*, *J. Phys. Chem. C* (2008)[130]

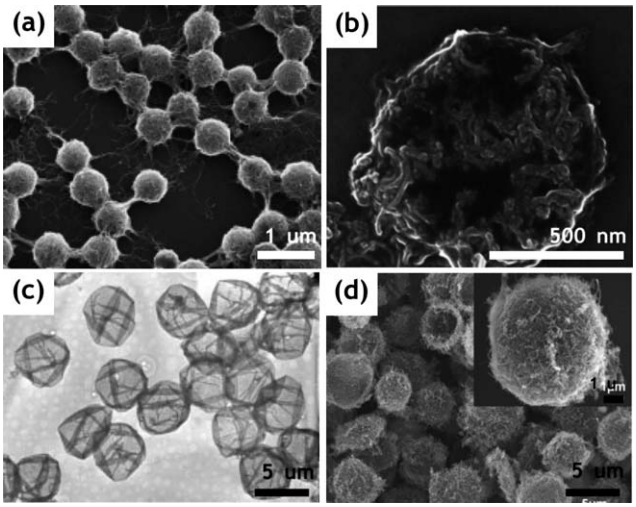

Fig. 16 (a) A SEM image of PS/CNT/PDDA core-shell composites before the removal of the PS templates; (b) a SEM image showing a collapsed CNT/PDDA hollow sphere after removal of the PS template shown in (a); (c) a TEM image of MWNT/PAH/PSS hollow capsules after removing MF template cores; (d) a SEM image of titania-reinforced CNT/PDDA hollow spheres assembled by the LbL deposition on PS templates. (Reprinted with permission from ref. 124,126 and 127, Ji *et al.*, *Chem. Comm.*, 2006, 1206; Copyright© The Royal Society of Chemistry, Zhao *et al.*, *Marcomol. Rapid Comm.*, 2004, **25**, 2014; Copyright© Wiley, Correa-Duarte *et al.*, *Chem. Mater.*, 2005, **17**, 3268; Copyright© The American Chemical Society.)

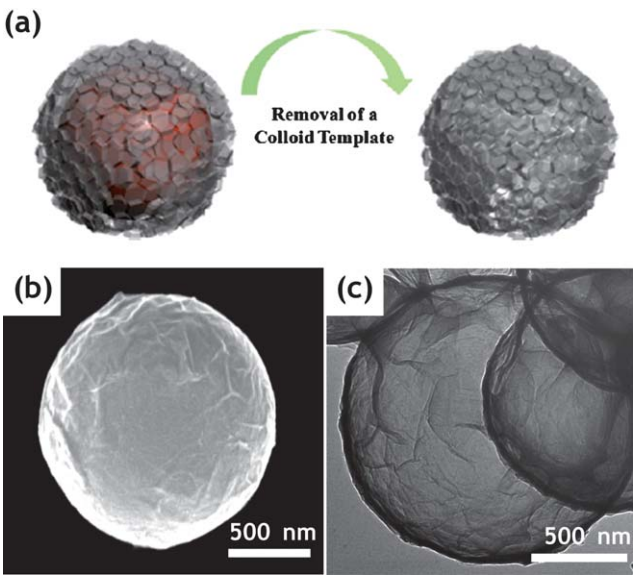

Fig. 17 (a) A schematic illustration of the construction of graphene-based hollow capsules. (b) A SEM image of a core-shell composite particle containing 3 bilayers of graphene oxide sheets on the 1 μm-sized PS template before the removal of the core template. (c) A TEM image of graphene-based hollow capsules containing 3 bilayers obtained after removing the PS templates in (b) with treatment with THF.

deposition. For example, we prepared the rGO hollow capsules containing gold nanoparticles in the interstitial layers of rGOs. The positively charged 4-(dimethylamino)pyridine (DMAP)-coated gold nanoparticles (AuNPs) were easily assembled with rGO–COO^- to form stable graphene/NP hybrid multilayer films with high Au NP density. Using a relevant modification of the LbL process with the conventional traditional bilayer format, positively charged Au NPs have been incorporated in every tetralayer of $(rGO–NH_3^+/rGO–COO^-/Au\ NPs/rGO–COO^-)_n$ multilayers, followed by the PS template removal to yield free-standing hollow rGO capsules containing high density Au NPs, as shown in Fig. 18. Another example is the attempt to incorporate quantum dots (CdS@ZnS QDs with green emission) into the graphene hollow shells based on the ligand-exchange step with cysteine to form hydrophilic positively charged quantum dots. Positively charged QDs were then deposited with the typical bilayer format, replacing the $GO–NH_3^+$, followed by the PS template removal to form $(QD/GO–COO^-)$ hollow capsules. Bright green fluorescent emission was observed in the bulk sample under UV lamp, and individual hollow capsules with green-emission were confirmed by a confocal laser scanning microscope (CLSM) (Fig. 18c and d).

Although there have been many reports on organic and/or inorganic hollow spheres for drug delivery and biomarkers, there has not been much attempt to use hollow structures based on carbon materials for such biomedical applications. CNTs or graphene-based hollow spheres also have potential to be used on traditional capsule applications; furthermore, we firmly believe that the concept of carbon-based hollow capsules would open up new areas of applications by fully exploiting their superb electronic and conductive properties.

5. Conclusion: emerging applications and outlook

The LbL assembly presents a class of hybrid materials that have enormous potential applications in many fields of science and

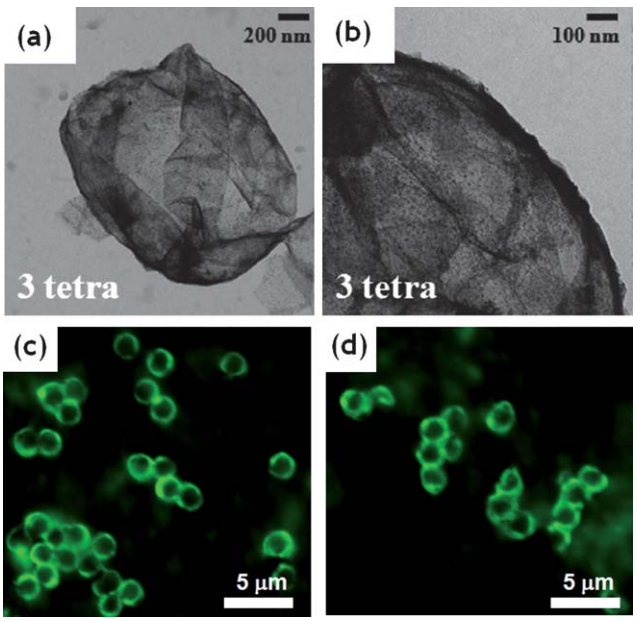

Fig. 18 (a) A TEM image of graphene-based capsule containing 3 tetralayers $(rGO–NH_3^+/rGO–COO^-/AuNPs/rGO–COO^-)_3$. (b) A magnified image of (a). (c) A confocal laser scanning microscopic (CLSM) image of core-shell composite particles containing GO and quantum dots (with green emission) before the removal of core templates. (d) A CLSM image of GO/quantum dots composite hollow capsules after removing the core templates.

engineering, owing to their tailorable structure, compositions, and tunable properties. In this Feature Article, we limit ourselves to an overview of the use of carbon-based nanomaterials in nanostructured films and capsules prepared by the LbL assembly focusing on the recent advancements in electronics, energy storage and conversion, sensing, and biotechnologies. Beyond the examples presented in this article, we anticipate many more exciting applications of utilizing the LbL films and capsules based on carbon nanomaterial in mechanical composites, environmental, biological, and biomedical applications in the near future.

As the integration with carbon nanomaterials based on the LbL assembly is gathering new perspectives and also finding many new applications, the following challenges need to be addressed: first, the most common protocol of incorporating the carbon materials into the LbL assembly is through the chemical modification of graphitic layers, which inevitably introduces the surface defects and sacrifices desirable electronic properties to some extent. Therefore, future endeavors should be focused on the development of a protocol that can even surpass the current protocols of the treatment on carbon nanomaterials. Second, the scale-up and development of new techniques for the assembly of carbon materials with fine tuning capability of film properties are still required from both theoretical and experimental aspects in order to bring this technique beyond the laboratory scale and move more toward the industrialized setup. Integrating carbon nanomaterials to fully utilize their unique physical, chemical, and electrical properties, the LbL assembly would improve the development of further fabrication techniques that will enable the precise control of these characteristic features with its simplicity and versatility.

Acknowledgements

This research was supported by the WCU (World Class University) program through the Korea Science and Engineering Foundation funded by the Ministry of Education, Science and Technology (R31-2008-000-20012-0) and the National Research Foundation of Korea Grant funded by the Korean Government (MEST) (The National Creative Research Initiative Program for "Intelligent Hybrids Research Center" 2010-0018290, 2010-0003219).

References

1 T. W. Ebbesen and P. M. Ajayan, *Nature*, 1992, **358**, 220–222.
2 A. P. Alivisatos, K. P. Johnsson, X. G. Peng, T. E. Wilson, C. J. Loweth, M. P. Bruchez and P. G. Schultz, *Nature*, 1996, **382**, 609–611.
3 G. A. J. Amaratunga, M. Chhowalla, C. J. Kiely, I. Alexandrou, R. Aharonov and R. M. Devenish, *Nature*, 1996, **383**, 321–323.
4 M. Li, E. Dujardin, S. Mann and Alivisatos, *Chem. Commun.*, 2005, 4952–4954.
5 A. V. Krasheninnikov and F. Banhart, *Nat. Mater.*, 2007, **6**, 723–733.
6 R. K. Iler, *J. Colloid Interface Sci.*, 1966, **21**, 569–594.
7 G. Decher, *Science*, 1997, **277**, 1232–1237.
8 F. Caruso, R. A. Caruso and H. Mohwald, *Science*, 1998, **282**, 1111–1114.
9 C. Lee, I. Kim, H. Shin, S. Kim and J. Cho, *Nat. Nanotechnol.*, 2010, **21**, 185704–185710.
10 T. Nakashima, J. A. Zhu, M. Qin, S. S. Ho and N. A. Kotov, *Nanoscale*, 2010, **2**, 2084–2090.
11 J. F. Rusling, E. G. Hvastkovs, D. O. Hull and J. B. Schenkman, *Chem. Commun.*, 2008, 141–154.
12 A. M. Yu, I. Gentle, G. Q. Lu and F. Caruso, *Chem. Commun.*, 2006, 2150–2152.
13 J. Hong, W. K. Bae, H. Lee, S. Oh, K. Char, F. Caruso and J. Cho, *Adv. Mater.*, 2007, **19**, 4364–4369.
14 J. Hong, K. Char and B. S. Kim, *J. Phys. Chem. Lett.*, 2010, **1**, 3442–3445.
15 V. Kozlovskaya, E. Kharlampieva, I. Drachuk, D. Cheng and V. V. Tsukruk, *Soft Matter*, 2010, **6**, 3596–3608.
16 D. M. Guldi, I. Zilbermann, G. A. Anderson, K. Kordatos, M. Prato, R. Tafuro and L. Valli, *J. Mater. Chem.*, 2004, **14**, 303–309.
17 M. Zhang, L. Sua and L. Mao, *Carbon*, 2006, **44**, 276–283.
18 S. W. Lee, J. Kim, S. Chen, P. T. Hammond and Y. Shao-Horn, *ACS Nano*, 2010, **4**, 3889–3896.
19 B. S. Kong, J. X. Geng and H. T. Jung, *Chem. Commun.*, 2009, 2174–2176.
20 S. Bae, H. Kim, Y. Lee, X. F. Xu, J. S. Park, Y. Zheng, J. Balakrishnan, T. Lei, H. R. Kim, Y. I. Song, Y. J. Kim, K. S. Kim, B. Ozyilmaz, J. H. Ahn, B. H. Hong and S. Iijima, *Nat. Nanotechnol.*, 2010, **5**, 574–578.
21 Y. Zhu and J. M. Tour, *Nano Lett.*, 2010, **10**, 4356–4362.
22 A. K. Geim and K. S. Novoselov, *Nat. Mater.*, 2007, **6**, 183–191.
23 F. Caruso, *Adv. Mater.*, 2001, **13**, 11–22.
24 P. T. Hammond, *Adv. Mater.*, 2004, **16**, 1271–1293.
25 J. L. Lutkenhaus and P. T. Hammond, *Soft Matter*, 2007, **3**, 804–816.
26 X. Zhang, H. Chen and H. Y. Zhang, *Chem. Commun.*, 2007, 1395–1405.
27 J. B. Schlenoff, *Langmuir*, 2009, **25**, 14007–14010.
28 P. Podsiadlo, B. S. Shim and N. A. Kotov, *Coord. Chem. Rev.*, 2009, **253**, 2835–2851.
29 R. K. Iler, *J. Am. Ceram. Soc.*, 1964, **47**, 194–198.
30 N. S. Zacharia, D. M. DeLongchamp, M. Modestino and P. T. Hammond, *Macromolecules*, 2007, **40**, 1598–1603.
31 H. S. Silva and P. B. Miranda, *J. Phys. Chem. B*, 2009, **113**, 10068–10071.
32 D. Lee, M. F. Rubner and R. E. Cohen, *Nano Lett.*, 2006, **6**, 2305–2312.
33 S. W. Lee, N. Yabuuchi, B. M. Gallant, S. Chen, B. S. Kim, P. T. Hammond and Y. Shao-Horn, *Nat. Nanotechnol.*, 2010, **5**, 531–537.
34 Z. Y. Tang, Z. L. Zhang, Y. Wang, S. C. Glotzer and N. A. Kotov, *Science*, 2006, **314**, 274–278.
35 B. Qi, X. Tong and Y. Zhao, *Macromolecules*, 2006, **39**, 5714–5719.
36 B. S. Kim, S. W. Park and P. T. Hammond, *ACS Nano*, 2008, **2**, 386–392.
37 J. Cho, J. Hong, K. Char and F. Caruso, *J. Am. Chem. Soc.*, 2006, **128**, 9935–9942.
38 L. Richert, P. Lavalle, E. Payan, X. Z. Shu, G. D. Prestwich, J.-F. Stoltz, P. Schaaf, J.-C. Voegel and C. Picart, *Langmuir*, 2004, **20**, 448–458.
39 J. Chluba, J.-C. Voegel, G. Decher, P. Erbacher, P. Schaaf and J. Ogier, *Biomacromolecules*, 2001, **2**, 800–805.
40 F. Cavalieri, A. Postma, L. Lee and F. Caruso, *ACS Nano*, 2009, **3**, 234–240.
41 K. T. Nam, D.-W. Kim, P. J. Yoo, N. Meethong, P. T. Hammond, Y.-M. Chiang and A. M. Belcher, *Science*, 2006, **312**, 885–888.
42 D. E. Bergbreiter and B. S. Chance, *Macromolecules*, 2007, **40**, 5337–5343.
43 Y. Zhang, H. He, C. Gao and J. Y. Wu, *Langmuir*, 2009, **25**, 5814–5824.
44 J. Choi and M. F. Rubner, *Macromolecules*, 2005, **38**, 116–124.
45 K. Itano, J. Y. Choi and M. F. Rubner, *Macromolecules*, 2005, **38**, 3450–3460.
46 J. Cho, K. Char, J. D. Hong and K. B. Lee, *Adv. Mater.*, 2001, **13**, 1076–1078.
47 J. B. Schlenoff, S. T. Dubas and T. Farhat, *Langmuir*, 2000, **16**, 9968–9969.
48 V. Z. Poenitzsch, D. C. Winters, H. Xie, G. R. Dieckmann, A. B. Dalton and I. H. Musselman, *J. Am. Chem. Soc.*, 2007, **129**, 14724–14732.

49 V. A. Sinani, M. K. Gheith, A. A. Yaroslavov, A. A. Rakhnyanskaya, K. Sun, A. A. Mamedov, J. P. Wicksted and N. A. Kotov, *J. Am. Chem. Soc.*, 2005, **127**, 3463–3472.
50 D. M. Guldi, F. Pellarini, M. Prato, C. Granito and L. Troisi, *Nano Lett.*, 2002, **2**, 965–968.
51 S. W. Lee, B. S. Kim, S. Chen, Y. Shao-Horn and P. T. Hammond, *J. Am. Chem. Soc.*, 2009, **131**, 671–679.
52 W. S. Hummers and R. E. Offeman, *J. Am. Chem. Soc.*, 1958, **80**, 1339.
53 K. S. Novoselov, A. K. Geim, S. V. Morozov, D. Jiang, Y. Zhang, S. V. Dubonos, I. V. Grigorieva and A. A. Firsov, *Science*, 2004, **306**, 666–669.
54 D. Li, M. B. Muller, S. Gilje, R. B. Kaner and G. G. Wallace, *Nat. Nanotechnol.*, 2008, **3**, 101–105.
55 N. I. Kovtyukhova, P. J. Ollivier, B. R. Martin, T. E. Mallouk, S. E. Chizhik, E. V. Buzaneva and A. D. Gorchinskiy, *Chem. Mater.*, 1999, **11**, 771–778.
56 T. K. Hong, D. W. Lee, H. J. Choi, H. S. Shin and B. S. Kim, *ACS Nano*, 2010, **4**, 3861–3868.
57 M. Eckle and G. Decher, *Nano Lett.*, 2001, **1**, 45–49.
58 J.-A. He, R. Mosurkal, L. A. Samuelson, L. Li and J. Kumar, *Langmuir*, 2003, **19**, 2169–2174.
59 K. Ariga, J. P. Hill and Q. Ji, *Phys. Chem. Chem. Phys.*, 2007, **9**, 2319–2340.
60 E. Jan and N. A. Kotov, *Nano Lett.*, 2007, **7**, 1123–1128.
61 J. Wu, Q. Tang, H. Sun, J. Lin, H. Ao, M. Huang and Y. Huang, *Langmuir*, 2008, **24**, 4800–4805.
62 B.-S. Kong, J. Geng and H.-T. Jung, *Chem. Commun.*, 2009, 2174–2176.
63 J. J. Yoo, K. Balakrishnan, J. Huang, V. Meunier, B. G. Sumpter, A. Srivastava, M. Conway, A. L. Mohana Reddy, J. Yu, R. Vajtai and P. M. Ajayan, *Nano Lett.*, 2011, **11**, 1423–1427.
64 N. A. Kotov, I. Dekany and J. H. Fendler, *Adv. Mater.*, 1996, **8**, 637–641.
65 B. S. Shim, J. Zhu, E. Jan, K. Critchley and N. A. Kotov, *ACS Nano*, 2010, **4**, 3725–3734.
66 W. Xue, Y. Lui and T. Cui, *Appl. Phys. Lett.*, 2006, **89**, 163512.
67 M. Lu, D. J. Lee, W. Xue and T. H. Cui, *Sens. Actuators, A*, 2009, **150**, 280–285.
68 D. W. Lee, T.-K. Hong, D. Kang, J. Lee, M. Heo, J. Y. Kim, B.-S. Kim and H. S. Shin, *J. Mater. Chem.*, 2011, **21**, 3438–3442.
69 X. Yu, R. Rajamani, K. A. Stelson and T. Cui, *Surf. Coat. Technol.*, 2008, **202**, 2002–2007.
70 X. Yu, R. Rajamani, K. A. Stelson and T. Cui, *Sens. Actuators, A*, 2006, **132**, 626–631.
71 T. A. Blizzard, F. DiNinno, J. D. Morgan, J. Y. Wu, H. Y. Chen, S. Kim, W. Chan, E. T. Birzin, Y. T. Yang, L. Y. Pai, Z. Zhang, E. C. Hayes, C. A. DaSilva, W. Tang, S. P. Rohrer, J. M. Schaeffer and M. L. Hammond, *Bioorg. Med. Chem. Lett.*, 2004, **14**, 3865–3868.
72 M. N. Zhang, K. P. Gong, H. W. Zhang and L. Q. Mao, *Biosens. Bioelectron.*, 2005, **20**, 1270–1276.
73 J. Kim, S. W. Lee, P. T. Hammond and Y. Shao-Horn, *Chem. Mater.*, 2009, **21**, 2993–3001.
74 J. J. Sun, H. Z. Zhao, Q. Z. Yang, J. Song and A. Xue, *Electrochim. Acta*, 2010, **55**, 3041–3047.
75 Z. H. Zhang, Y. F. Hu, H. B. Zhang, J. Cao and S. Z. Yao, *Chin. J. Chem.*, 2010, **68**, 431–436.
76 M. Michel, A. Taylor, R. Sekol, P. Podsiadlo, P. Ho, N. A. Kotov and L. Thompson, *Adv. Mater.*, 2007, **19**, 3859–3864.
77 L. Deng, F. Wang, H. J. Chen, L. Shang, L. Wang, T. Wang and S. J. Dong, *Biosens. Bioelectron.*, 2008, **24**, 329–333.
78 M. Zhou, L. Deng, D. Wen, L. Shang, L. H. Jin and S. J. Dong, *Biosens. Bioelectron.*, 2009, **24**, 2904–2908.
79 Z. C. Hu, J. J. Xu, Y. Tian, R. Peng, Y. Z. Xian, Q. Ran and L. T. Jin, *Electrochim. Acta*, 2009, **54**, 4056–4061.
80 B. S. Shim, W. Chen, C. Doty, C. L. Xu and N. A. Kotov, *Nano Lett.*, 2008, **8**, 4151–4157.
81 K. J. Loh, J. Kim, J. P. Lynch, N. W. S. Kam and N. A. Kotov, *Smart Mater. Struct.*, 2007, **16**, 429–438.
82 B. S. Kim, S. W. Lee, H. Yoon, M. S. Strano, Y. Shao-Horn and P. T. Hammond, *Chem. Mater.*, 2010, **22**, 4791–4797.
83 D. Nepal, S. Balasubramanian, A. L. Simonian and V. A. Davis, *Nano Lett.*, 2008, **8**, 1896–1901.
84 P. G. Su and Y. S. Chuang, *Sens. Actuators, B*, 2010, **145**, 521–526.
85 M. Olek, J. Ostrander, S. Jurga, H. Mohwald, N. A. Kotov, K. Kempa and M. Giersig, *Nano Lett.*, 2004, **4**, 1889–1895.
86 M. Zhang, L. Su and L. Mao, *Carbon*, 2006, **44**, 276–283.
87 Y. Zhang and J. B. Zheng, *Electrochim. Acta*, 2008, **54**, 749–754.
88 Z. Hu, J. Xu, Y. Tian, R. Peng, Y. Xian, Q. Ran and L. Jin, *Carbon*, 2010, **48**, 3729–3736.
89 Z.-Z. Zhu, G.-C. Wang, M.-Q. Sun, X.-W. Li and C.-Z. Li, *Electrochim. Acta*, 2011, **56**, 1366–1372.
90 G. M. A. Rahman, D. M. Guldi, R. Cagnoli, A. Mucci, L. Schenetti, L. Vaccari and M. Prato, *J. Am. Chem. Soc.*, 2005, **127**, 10051–10057.
91 Y. Wang, P. P. Joshi, K. L. Hobbs, M. B. Johnson and D. W. Schmidtke, *Langmuir*, 2006, **22**, 9776–9783.
92 B. S. Shim, J. Zhu, E. Jan, K. Critchley, S. S. Ho, P. Podsiadlo, K. Sun and N. A. Kotov, *ACS Nano*, 2009, **3**, 1711–1722.
93 V. Sgobba, A. Troeger, R. Cagnoli, A. Mateo-Alonso, M. Prato, F. Parenti, A. Mucci, L. Schenetti and D. M. Guldi, *J. Mater. Chem.*, 2009, **19**, 4319–4324.
94 K. E. Tettey, M. Q. Yee and D. Lee, *Langmuir*, 2010, **26**, 9974–9980.
95 H. R. Byon, S. W. Lee, S. Chen, P. T. Hammond and Y. Shao-Horn, *Carbon*, 2011, **49**, 457–467.
96 K. K. Manga, Y. Zhou, Y. Yan and K. P. Loh, *Adv. Funct. Mater.*, 2009, **19**, 3638–3643.
97 K. W. Putz, O. C. Compton, M. J. Palmeri, S. T. Nguyen and L. C. Brinson, *Adv. Funct. Mater.*, 2010, **20**, 3322–3329.
98 U. Lange, T. Hirsch, V. M. Mirsky and O. S. Wolfbeis, *Electrochim. Acta*, 2010, **56**, 3707–3712.
99 S. Mandal, M. Sathish, G. Saravanan, K. K. R. Datta, Q. Ji, J. P. Hill, H. Abe, I. Honma and K. Ariga, *J. Am. Chem. Soc.*, 2010, **132**, 14415–14417.
100 D. D. Kulkarni, I. Choi, S. S. Singamaneni and V. V. Tsukruk, *ACS Nano*, 2010, **4**, 4667–4676.
101 A. Rani, K. A. Oh, H. Koo, H. J. Lee and M. Park, *Appl. Surf. Sci.*, 2011, **257**, 4982–4989.
102 Z. Li, J. Wang, X. Liu, S. Liu, J. Ou and S. Yang, *J. Mater. Chem.*, 2011, **21**, 3397–3403.
103 A. S. Angelatos, B. Radt and F. Caruso, *J. Phys. Chem. B*, 2005, **109**, 3071–3076.
104 C. J. Martinez, B. Hockey, C. B. Montgomery and S. Semancik, *Langmuir*, 2005, **21**, 7937–7944.
105 Z. Wang, L. Qian, X. Wang, F. Yang and X. Yang, *Colloids Surf., A*, 2008, **326**, 29–36.
106 M.-K. Park, K. Onishi, J. Locklin, F. Caruso and R. C. Advincula, *Langmuir*, 2003, **19**, 8550–8554.
107 W. B. Stockton and M. F. Rubner, *Macromolecules*, 1997, **30**, 2717–2725.
108 T. Serizawa, S. Kamimura, N. Kawanishi and M. Akashi, *Langmuir*, 2002, **18**, 8381–8385.
109 T. Serizawa, K. Nanameki, K. Yamamoto and M. Akashi, *Macromolecules*, 2002, **35**, 2184–2189.
110 A. P. R. Johnston, E. S. Read and F. Caruso, *Nano Lett.*, 2005, **5**, 953–956.
111 F. Caruso, R. A. Caruso and H. Möhwald, *Chem. Mater.*, 1999, **11**, 3309–3314.
112 A. Yu, Y. Wang, E. Barlow and F. Caruso, *Adv. Mater.*, 2005, **17**, 1737–1741.
113 G. Schneider, G. Decher, N. Nerambourg, R. Praho, M. H. V. Werts and M. Blanchard-Desce, *Nano Lett.*, 2006, **6**, 530–536.
114 F. Cuomo, F. Lopez, M. G. Miguel and B. Lindman, *Langmuir*, 2010, **26**, 10555–10560.
115 H. Daiguji, E. Matsuoka and S. Muto, *Soft Matter*, 2010, **6**, 1892–1897.
116 H. W. Kroto, J. R. Heath, S. C. O'Brien, R. F. Curl and R. E. Smalley, *Nature*, 1985, **318**, 162–163.
117 T. Suzuki, Q. LI, K. C. Khemani, F. Wudl and Ö. Almarsson, *Science*, 1991, **254**, 1186–1188.
118 E. W. Wong, P. E. Sheehan and C. M. Lieber, *Science*, 1997, **277**, 1971–1975.
119 T. W. Odom, J.-L. Huang, P. Kim and C. M. Lieber, *Nature*, 1998, **391**, 62–64.
120 J. P. Salvetat, J. M. Bonard, N. H. Thomson, A. J. Kulik, L. Forró, W. Benoit and L. Zuppiroli, *Appl. Phys. A: Mater. Sci. Process.*, 1999, **69**, 255–260.

121 A. A. Balandin, S. Ghosh, W. Bao, I. Calizo, D. Teweldebrhan, F. Miao and C. N. Lau, *Nano Lett.*, 2008, **8**, 902–907.
122 K. I. Bolotin, K. J. Sikes, Z. Jiang, M. Klima, G. Fudenberg, J. Hone, P. Kim and H. L. Stormer, *Solid State Commun.*, 2008, **146**, 351–355.
123 C. Lee, X. Wei, J. W. Kysar and J. Hone, *Science*, 2008, **321**, 385–388.
124 L. Ji, J. Ma, C. Zhao, W. Wei, L. J. Ji, X. Wang, M. Yang, Y. Lu and Z. Yang, *Chem. Commun.*, 2006, 1206–1208.
125 V. Salgueirino-Maceira, M. A. Correa-Duarte and M. Farle, *Small*, 2005, **1**, 1073–1076.
126 Q. Zhao, C. Gao, J. Shen, Y. Li and X. Zhang, *Macromol. Rapid Commun.*, 2004, **25**, 2014–2018.
127 M. A. Correa-Duarte, A. Kosiorek, W. Kandulski, M. Giersig and L. M. Liz-Marzan, *Chem. Mater.*, 2005, **17**, 3268–3272.
128 M. Sano, A. Kamino, J. Okamura and S. Shinkai, *Nano Lett.*, 2002, **2**, 531–533.
129 K. Sugikawa, M. Numata, K. Kaneko, K. Sada and S. Shinkai, *Langmuir*, 2008, **24**, 13270–13275.
130 J. Shi, Z. Chen, Y. Qin and Z. X. Guo, *J. Phys. Chem. C*, 2008, **112**, 11617–11622.